Assessment of Long-Term Spatio-Temporal Radiofrequency Electromagnetic Field Exposure

Sam Aerts[1], Joe Wiart[2], Luc Martens[1], and Wout Joseph[1]

[1]Department of Information Technology, Ghent University / imec, Ghent, Belgium

[2]*Institut Mines-Telecom Telecom ParisTech, LTCI, Chaire C2m, Paris, France*

Abstract

As both the environment and telecommunications networks are inherently dynamic, our exposure to environmental radiofrequency (RF) electromagnetic fields (EMF) at an arbitrary location is not at all constant in time. In this study, more than a year's worth of measurement data collected in a fixed low-cost exposimeter network distributed over an urban environment was analysed and used to build, for the first time, a full spatio-temporal surrogate model of outdoor exposure to downlink Global System for Mobile Communications (GSM) and Universal Mobile Telecommunications System (UMTS) signals. Though no global trend was discovered over the measuring period, the difference in measured exposure between two instances could reach up to 42 dB (a factor 12,000 in power density). Furthermore, it was found that, taking into account the hour and day of the measurement, the accuracy of the surrogate model in the area under study was improved by up to 50% compared to models that neglect the daily temporal variability of the RF signals. However, further study is required to assess the extent to which the results obtained in the considered environment can be extrapolated to other geographic locations.

Keywords – spatio-temporal exposure assessment; telecommunications; radiofrequency electromagnetic fields; non-ionizing radiation

I Introduction

Wireless telecommunications technologies have become an indispensable and ubiquitous part of our everyday life. As these technologies continue to grow more diverse and complex, in order to satisfy our evermore increasing desire for connectivity, so does the range of radiofrequency (RF) electromagnetic fields (EMF) used to carry the signals. Although ambient levels of RF-EMF generally encountered in everyday circumstances remain well below established scientific limits (ICNIRP, 1998), their relentless presence in our society raises concerns that long-term exposure at low levels may be associated with various non-specific physical symptoms (Baliatsas et al., 2015) and ecological effects on fauna and flora (Cucurachi, 2013).

Over the last decades, a number of studies have aimed at characterising the environmental RF-EMF exposure using either personal or spot measurements performed during the day. However, while our exposure to environmental RF-EMF is not at all constant in time due to environmental changes and variations in the number of active users (as well as the nature of their activity) in telecommunications networks (Joseph et al., 2009; Joseph and Verloock, 2010), these studies tend to neglect the temporal dimension (e.g., Frei et al., 2009; Aerts et al., 2013a; 2013b; 2017; Beekhuizen et al., 2013).

In spite of RF-EMF monitoring systems installed in various cities in Europe, such as in Greece (Gotsis et al., 2008), Italy (Troisi et al., 2008), and Portugal (Oliveira et al., 2007), published temporal analyses are scarce: the short-term variability of environmental RF-EMF – i.e., the variation between day and night-time as well as between the different days of the week – has been studied by e.g., Joseph et al. (2009), Joseph and Verloock (2010), Manassas et al. (2012), Mahfouz et al. (2012, 2013), Miclaus et al. (2013), Vermeeren et al. (2013), and Verloock et al. (2014), while long-term analyses have been performed by e.g., Rowley and Joyner (2012), Urbinello et al. (2014), and Tomitsch and Dechant (2015), using repeated measurements instead of monitoring networks. More importantly, detailed temporal information has yet to be included in RF-EMF surrogate modelling (Aerts et al., 2013a; 2013b; 2017).

In this paper, the impact of the temporal variability of telecommunications signals on outdoor RF-EMF exposure characterization is investigated. During more than a year, measurements of three downlink telecommunications signals – i.e., from base station to user device – were collected in a low-cost exposimeter network within an urban setting. First, the potential errors of using measurements at single instances were determined. Next, from this vast set of data, for the first time, a full spatio-temporal surrogate model could be built. And finally, global profiles of the daily variation of the signals were composed, which were used to quantify the improvement of adding the temporal dimension to established RF-EMF surrogate modelling techniques.

II Materials & Methods

Long-term measurements of downlink telecommunications signals (i.e., the signals from base stations to personal devices) were gathered in a monitoring network comprising a number of fixed exposimeters. The analysis consisted in (a) calculating the variability of the signals over the entire measuring period in order to quantify the possible errors induced in surrogate models by assuming the downlink signal strength is constant in time; (b) determining the average variation of the signals during a single day (i.e., from 00:00 to 23:59); and (c) using this information to scale measurements taken at different times during the day (mimicking a real-life measurement campaign) to a single time instance in order to obtain an accurate surrogate model of the RF exposure at that single instance.

II.1 Monitoring Network

In the city of Santander, Spain, an Internet-of-Things (IoT) platform (SmartSantander; http://smartsantander.eu/) has been deployed consisting of a network of IoT nodes which continuously measure various environmental parameters, such as temperature and CO_2. The area covered by the SmartSantander platform has a size of 0.4 km by 1.4 km. Recently, in the EU-FP7 LEXNET project, RF-EMF exposimeters have been added to this IoT platform (Diez et al., 2014), attached to masts at a height of 3 m. These devices were specifically designed to measure the environmental exposure (quantified by the electric field strength E, in V/m) induced by the three most-used telecommunications technologies (i.e., Global System for Mobile Communications (GSM) at 900 MHz (GSM900) and 1800 MHz (GSM1800), and Universal Mobile Telecommunications System (UMTS) at 2100 MHz). Moreover, they were developed for large-scale deployment, thus as cost-efficiently as possible. Frequency bands specifically used by fourth generation (4G) Long Term Evolution (LTE) were not included, as this technology was not yet in use when the exposimeters were installed in 2014 (Diez et al., 2014).

II.2 Exposimeter Measurements

A measurement of a certain frequency band was performed by sampling the output voltage (0 V to 3.3 V) and then calculating the median or maximum value of the acquired samples to obtain a single output value. The treatment and number of samples depended on the band, and was determined based on the calibration process (Diez et al., 2014). Then, this output value was converted to an electric-field strength within the range 5 mV/m to 5 V/m, using the exposimeter's antenna factor (AF) (Diez et al., 2014). Each of the considered frequency bands were alternately selected using an RF switch, and the nominal sample collection time (one value for each band)

was either 5 or 10 minutes, depending on the specific exposimeter. This study focused on the telecommunications bands and also calculated the total electric-field strength as,

$$E_{total} = \sqrt{E_{GSM900}^2 + E_{GSM1800}^2 + E_{UMTS}^2}, \quad (1)$$

with E_i the electric-field strength measured in band i (GSM900, GSM1800, or UMTS – all downlink).

Finally, the data used in this study were collected during 14 months – between 9th of December, 2015, and the 15th of February, 2017.

II.3 Analysis of the Measurements

II.3.1 Temporal variability

At every exposimeter measurement position, the variability of the considered signals over the entire measuring period was determined. More specifically, the maximum (V_{max}) and 90-percent variability (V_{90}) were determined, using

$$V_{max}(T) = 20\log_{10}\left(\frac{\max\limits_{t\in T}(E(t))}{\min\limits_{t\in T}(E(t))}\right), \quad (2)$$

$$V_{90}(T) = 20\log_{10}\left(\frac{\mathrm{p}_{95}\limits_{t\in T}(E(t))}{\mathrm{p}_{5}\limits_{t\in T}(E(t))}\right), \quad (3)$$

where max(E) and min(E) are the maximum and minimum, and $p_x(E)$ the x-th percentile of the electric-field values collected in a specific frequency band during the considered measuring period T.

V_{max} and V_{90} provide estimates of the error induced by neglecting the temporal dimension, which is useful for instantaneous, non-repeated measurements with a similar device.

II.3.2 Temporal profiles

The next step consisted in identifying the average trends of the signal strength over a certain period of time, which, in this case, was either a day (i.e., the variation of the signal between 00:00 and 23:59, averaged over all measurement days) or a week (i.e., the daily variation depending on the day of the week).

In order to obtain a smoother profile, and because the median time between measurements was not the same for all exposimeters, hour-aggregated averages $E(h)$ (with h a year-month-day-hour instance, for example '2016-12-24 19:00') were used in this analysis – i.e., the mean of the values collected between HH:00 and HH:59 (with HH = 00 to 23) on the same day d.

Furthermore, to rule out any potential bias due to long-term variations in the signal (e.g., due to changes in the network infrastructure), the relative variation η of the signal compared to the daily average was calculated,

$$\eta(h) = \frac{E(h)^2}{\underset{h \in d}{\text{mean}}(E(h)^2)} \tag{4}$$

Finally, by aggregating and averaging all these relative values per time slot, defined as (a) *hour* (HH, with HH = 00 to 23), or (b) *day-hour* (DDD-HH, with DDD = MON to SUN, or Monday to Sunday), *temporal profiles* were created.

II.4 Spatio-Temporal Exposure Maps

In the final step, the possibility was investigated of creating, at any instance of time h, a spatial surrogate model of the RF-EMF exposure using a subset of size N of the collected measurements, i.e., the electric-field values $E(h_i, \boldsymbol{X_i})$ (i = 1 … N) collected at instances h_i and locations $\boldsymbol{X_i}$. Within this subset, the same instances as well as the same locations can occur multiple times, though not simultaneously, mimicking a real-life measurement campaign using multiple measurement devices (of the same type) at the same time and possibly returning to the same locations at different instances. By rescaling the samples $E(h_i, \boldsymbol{X_i})$ to the considered time instance h according to the identified temporal profiles and subsequently interpolating them over the study area using ordinary Kriging (Matheron, 1963), a surrogate model at h can be obtained. Random samples taken at the same location were averaged to retain only one value, and each surrogate model was built 100 times using different random subsets.

To assess the validity of this spatio-temporal modelling, first, the 'correct' spatial model at h was constructed using the exact information available at that instance, by interpolating the spatial measurements taken at time instance h at every available location, thus creating *reference slices*. Then, three types of models were built from subsets $E(h_i, \boldsymbol{X_i})$: a non-adjusted model (no rescaling), an hour-adjusted model (rescaling according to the *hour* profile), and a day-hour-adjusted model (rescaling according to the *day-hour* profile). All three types were compared to the reference slices by calculating the *temporal bias* β (i.e., the relative error of the model compared to the reference slice), defined as

$$\beta_{model}(h) = \underset{\boldsymbol{X} \in \boldsymbol{area}}{\text{mean}} \left(\frac{E_{model}(h, \boldsymbol{X})^2 - E_{ref}(h, \boldsymbol{X})^2}{E_{ref}(h, \boldsymbol{X})^2} \right), \tag{5}$$

where $\boldsymbol{X}$ represents an interpolation grid point, E_{model} the electric-field strength predicted by the surrogate model constructed using the random set of (non-)adjusted measurement values taken at different moments, and E_{ref} the electric-field strength predicted by the 'correct' model or reference slice, built from the exact information at time instance h.

III Results & Discussion

III.1 Analysis of the Exposimeter Network Measurements

The SmartSantander exposimeter network consisted of 36 exposimeters that were active during any period of time between 09-12-15 and 15-02-17. A summary of the measuring periods and measurement results is given in Supplementary Materials – Table 1. Unfortunately, none of the exposimeters worked consistently. For all further analysis, only the exposimeters with an adequate amount of measurements were retained to create temporal profiles (i.e., 50 days, or n_m = 14,400 or 7,200 at respective measurement collection times of 5 min and 10 min) and removed the (four) malfunctioning devices from the analysis. The locations and IDs (corresponding to Supplementary Materials – Table 1) of the 32 considered exposimeters of the network considered in this study are shown in Figure 1.

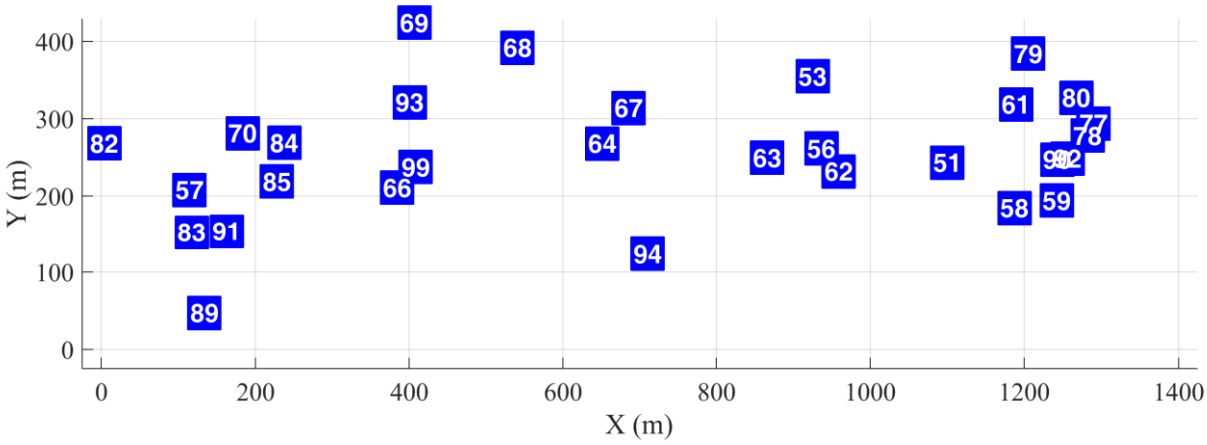

Figure 1: The (X,Y)-locations and IDs of the exposimeters considered in this study (see Supplementary Materials – Table 1 for a summary of the measurements).

Across all measurement devices, the largest number of samples collected was 93,768 ('64', in Figure 1), which accounted for 326 days. Averaged over the exposimeters' active measuring periods, E_{signal} varied between 8 mV/m ('78', UMTS) and 371 mV/m ('82', GSM1800) (Supplementary Materials – Table 1). The average electric-field strengths measured over the entire study area and measuring period (09-12-15 and 15-02-17) were 61 mV/m for GSM900, 99 mV/m for GSM1800, and 64 mV/m for UMTS. It should be noted, though, that only one electric-field component (vertical one) was measured by the exposimeter (Supplementary Materials – Table 1), so these values are underestimations.

It should be noted that, due to the nature of these measurements, compliance with ICNIRP reference levels could not be assessed.

III.1.1 Temporal variability of the signals

Figure 2 shows the ranges of the variability of the telecommunications (downlink) signals over the total assessment time of 14 months and over all 32 measurement locations. The maximum variability – and thus the potential error of a single exposimeter measurement, i.e., a measurement at one time instance as the proxy for the exposure at this location – was rather high, with median V_{max} of 16 to 21 dB (and 13 dB for E_{total}), and maximum V_{max} of up to 30 to 42 dB. The median 90% variability, on the other hand, was of the order of 10 times lower and quite the same for all signals (6 to 7 dB for the individual signals, and 5 dB for E_{total}). However, the range of variability was much broader for GSM1800 than for both GSM900 and UMTS, and overall, the values were higher for this band, with up to 37 dB even for V_{90}.

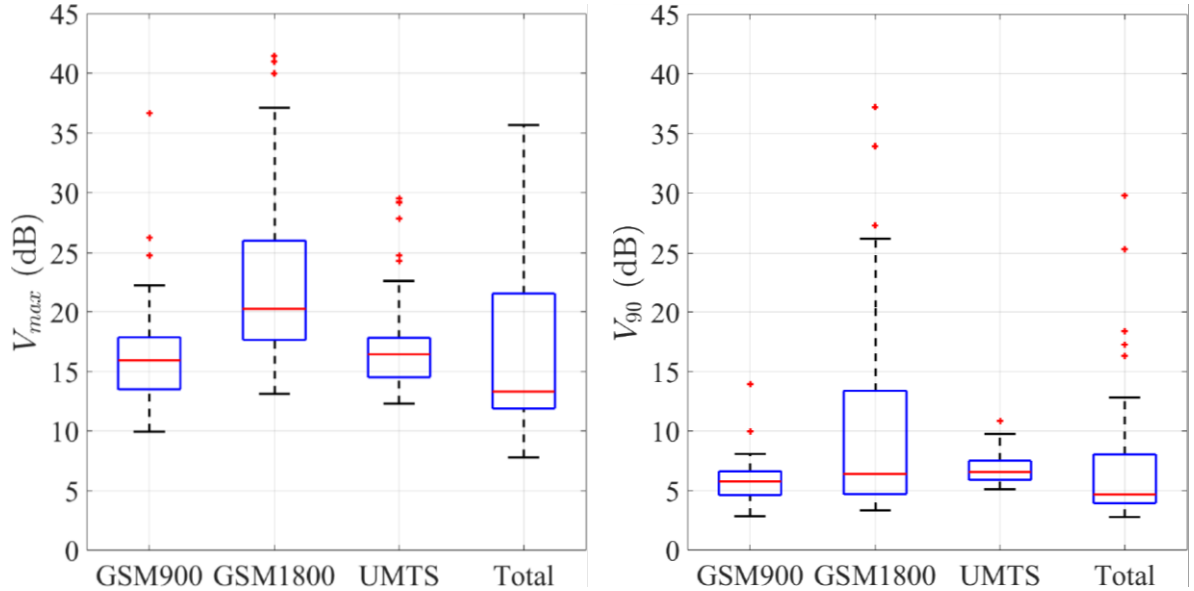

(a) V_{max} (b) V_{90}

Figure 2: (a) Maximum and (b) 90-percent temporal variability of the signals over the total assessment period (i.e., 09-12-2015 to 15-02-2017).

III.1.2 Temporal profiles

To illustrate the short-term temporal variation in the measured electric-field strength, in Figure 3(a), the relative total electric-field strength η_{total} (i.e., the ratio of the measured E_{total} to $E_{total,avg}$, the average electric-field strength measured over the day) measured at one location ('99') for a week (01-12-16 to 07-12-16) was plotted, and in Figure 3(b) η_{total} at the same location for one specific day (01-12-16).

In this specific case, a measurement at a single moment during this week could be off by -64% (η_{total} = 0.36; hour-aggregated: 0.40) up to +422% (η_{total} = 5.22; hour-aggregated: 2.83) compared to the average electric-field strength at that location, depending on the time and day of the measurement.

In order to mitigate this error induced by performing measurements at different time instances, temporal profiles were constructed. In Figure 4, the *location-aggregated day-hour profiles* , i.e., the variation of η per hour and day of the week averaged over all measurement devices, were plotted for each of the measured frequency bands, and in Figure 5, the *location-aggregated hour profiles* (for which the day of the week was disregarded) were plotted.

The daily variation in the UMTS band was the highest (Figures 4 and 5), although the extreme variations η were quite small (0.60 – 1.40). For GSM1800, as well as GSM900 and the total field, the electric-field strength hovered between $\pm 20\%$ of the daily average. Comparing weekdays, Monday to Thursday appeared to be fairly similar (Figure 4), though Friday (orange, Figure 4), Saturday (red), and Sunday (dark green) all boasted distinct variations. Furthermore, the weekend nights boasted higher variations η, the weekend mornings and afternoons lower η. Once again, these trends were more outspoken for UMTS than for the other signals.

The fact that the variation η remains so close to 1, in contrast to the high variability observed in the previous section, emphasizes the potential errors inherent to single, momentaneous measurements and justifies the use of hour-aggregated values in further analysis.

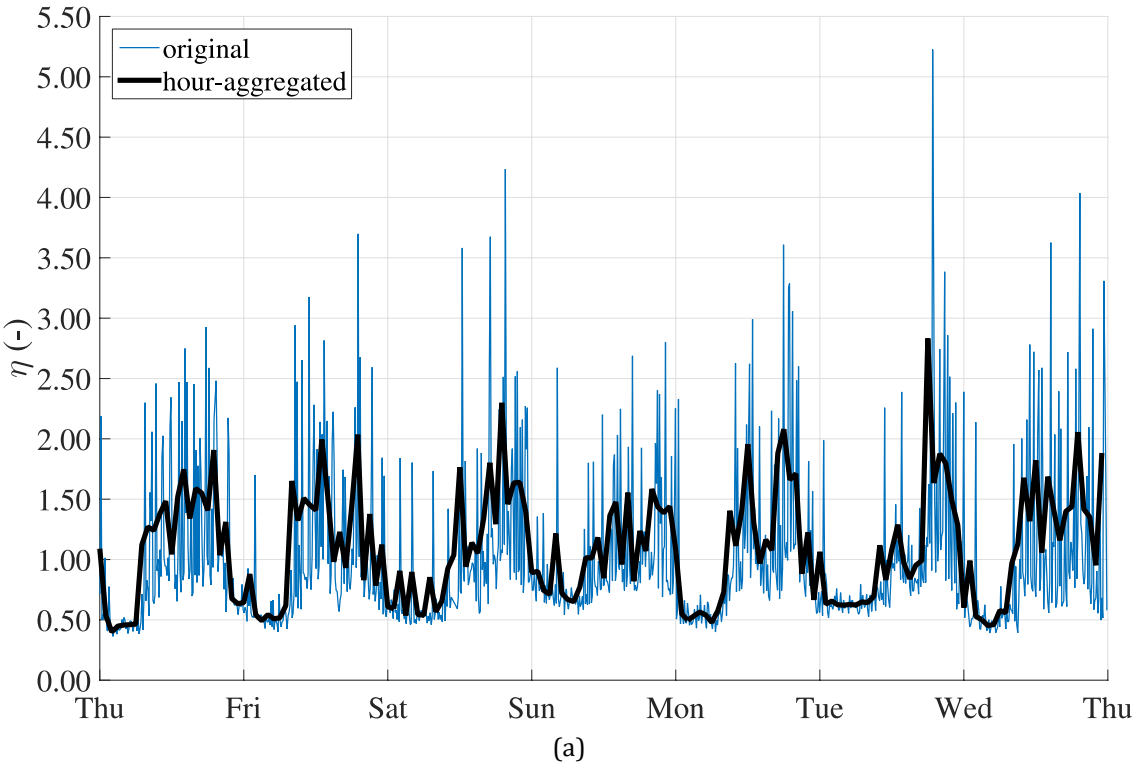

(a)

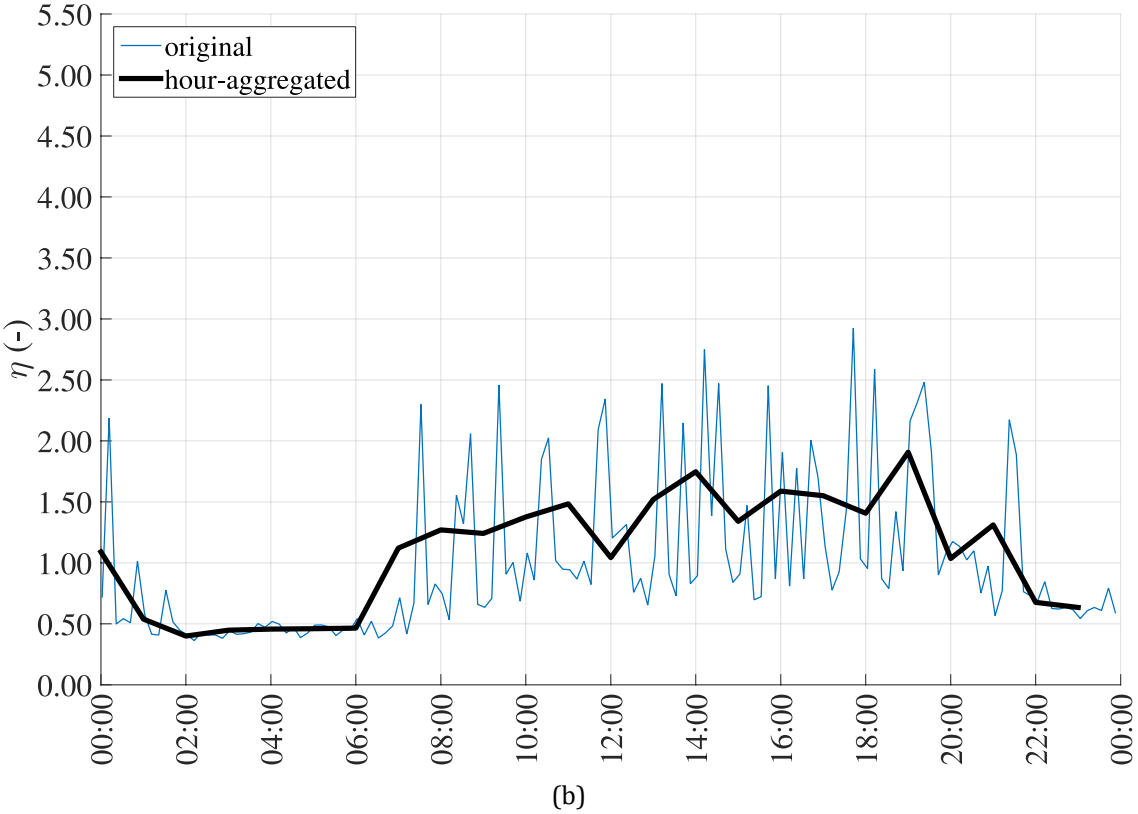

(b)

Figure 3: Relative total electric-field strength η_{total}, measured during (a) one week (01-12-16 to 07-12-16) and (b) one day (01-12-16).

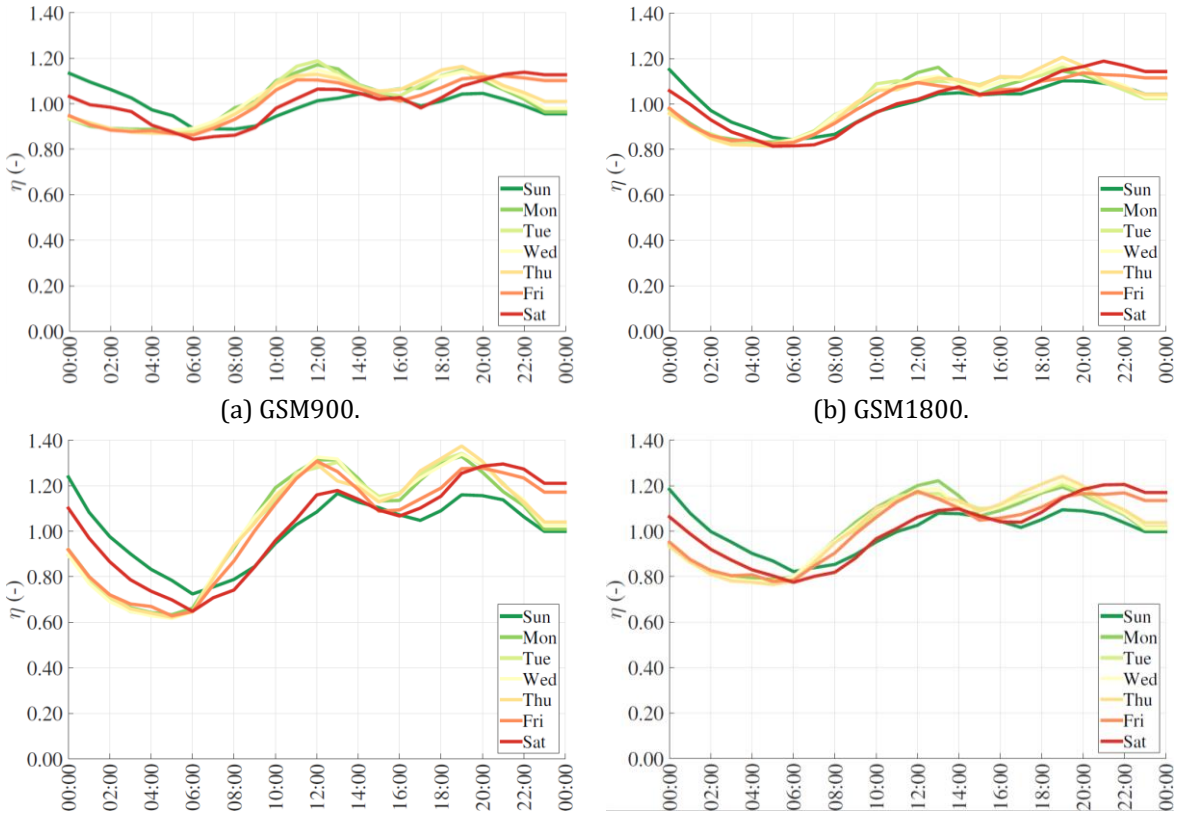

(a) GSM900. (b) GSM1800.

(c) UMTS. (d) Total.

*Figure 4: Location-aggregated **day-hour** profiles (used at all measurement locations).*

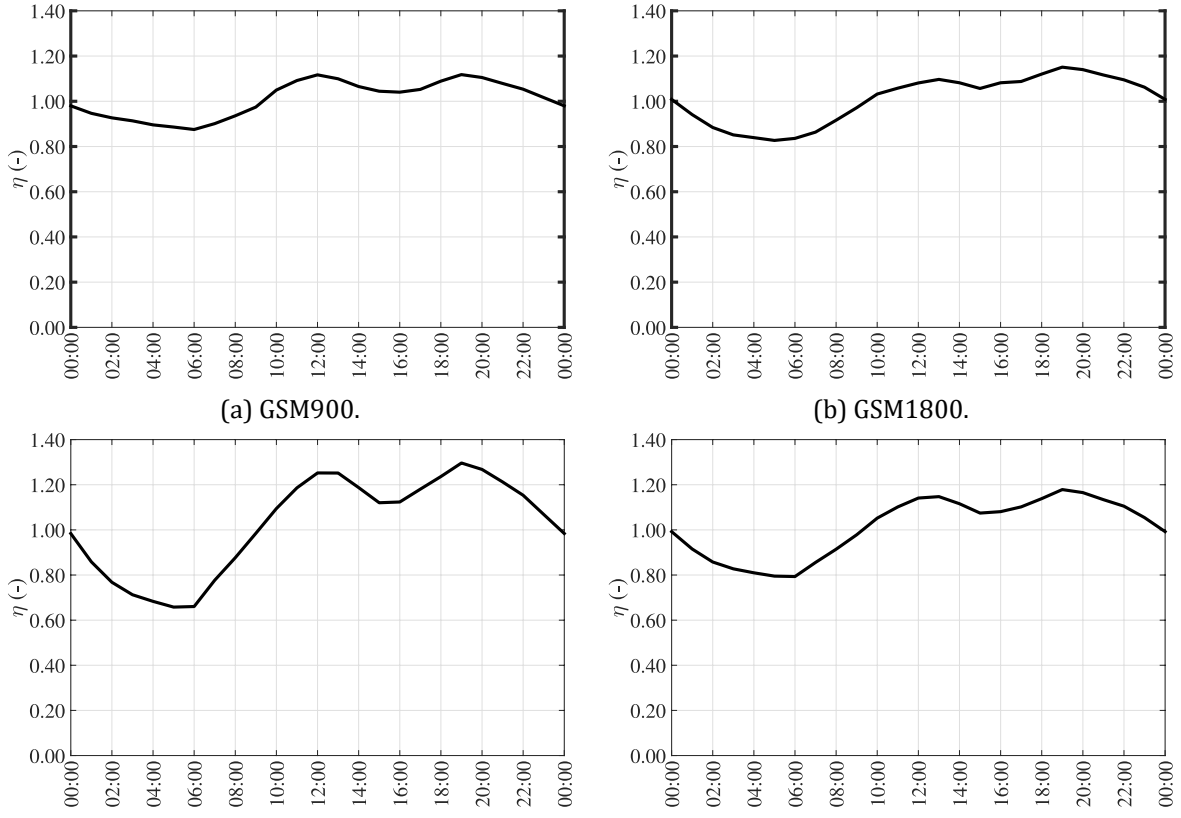

(a) GSM900. (b) GSM1800.

(c) UMTS. (d) Total.

*Figure 5: Location-aggregated **hour** profiles (used at all measurement locations).*

III.2 Spatio-Temporal Interpolation

For the final step of this study, a period of time was selected during which the majority of the exposimeters measured nearly continuously, namely from 01-12-16 (Thursday) to 07-12-16 (Wednesday). First, hourly models were constructed at each time instance ('reference slices').

For illustration, in Figure 6, a few slices for GSM900 are shown. To better illustrate the spatio-temporal variations, the electric-field strength is in log scale (dB V/m). Though the positions of local features (i.e., the regions of higher and lower levels) within the spatial distribution of E^{GSM900} remained fairly stable through time, the levels and the shape of the overall distribution clearly changed. This indicates that while the methodology introduced in Aerts et al. (2013b) is solid to locate hotspots, the overall accuracy of the exposure levels also depends on the time of measurement in comparison to the time of assessment. For example, an assessment of the exposure at 14:00 on Sunday will be inaccurate using measurements at 09:00 on Friday (Figure 6).

From this week, random sets of 100 hour-averaged measurement values were used to build surrogate models at each time instance *h* between 01-12-16 00:00 and 07-12-16 23:00, using (i) the non-adjusted values, (ii) the location-aggregated day-hour-adjusted values, and (iii) the location-aggregated hour-adjusted values. To quantify the usefulness of the introduced temporal profiles, for each time-instant *h*, the hourly models (reference slices) were subsequently compared with the (non-)adjusted surrogate models. The cumulative distribution functions (CDFs) of the introduced temporal bias are shown in Figure 7, and the median temporal biases listed in Table 1.

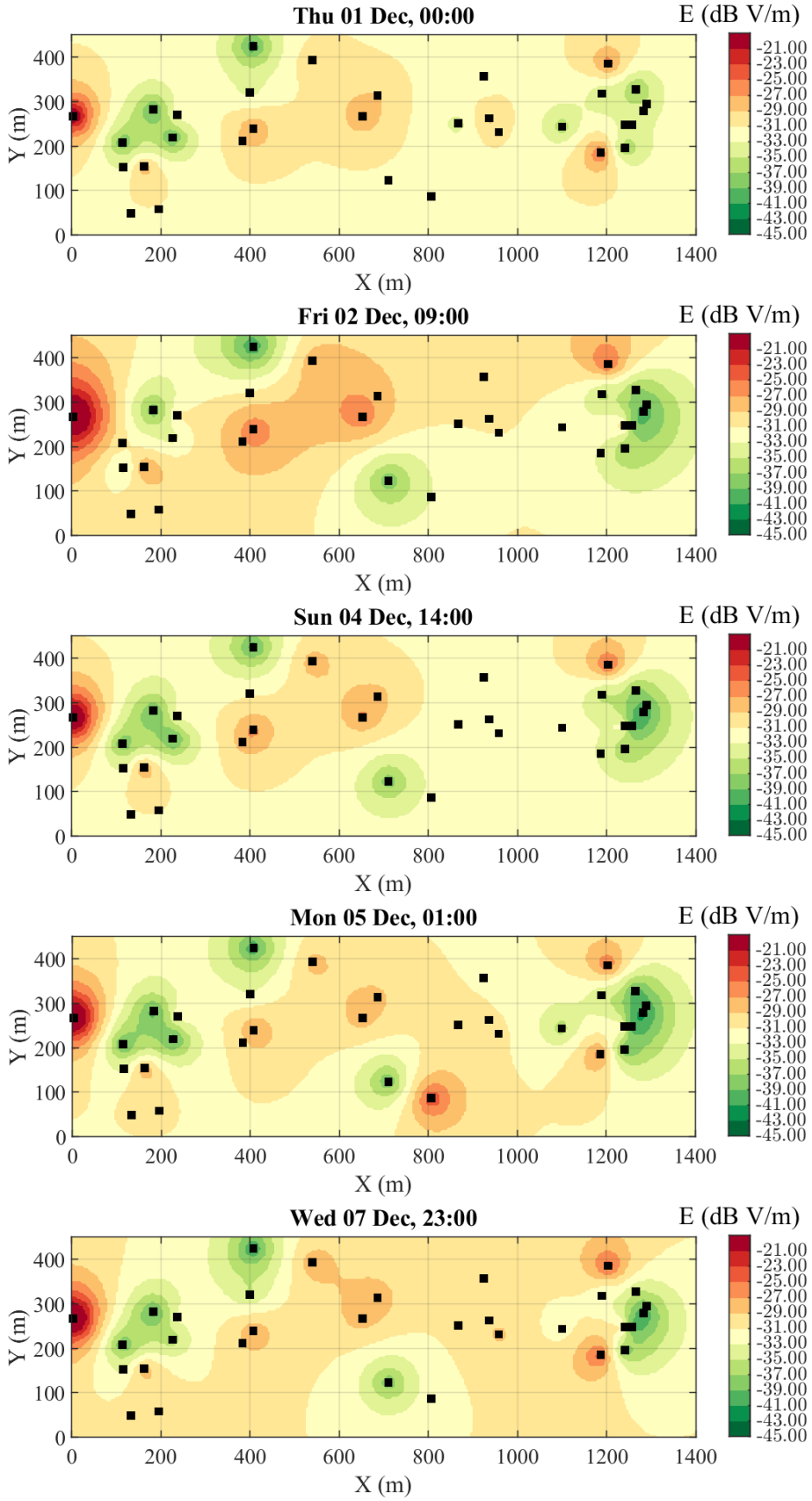

Figure 6: Surrogate models at different time instances (or reference slices) for GSM900 (downlink). The black squares indicate exposimeter locations (see Figure 1).

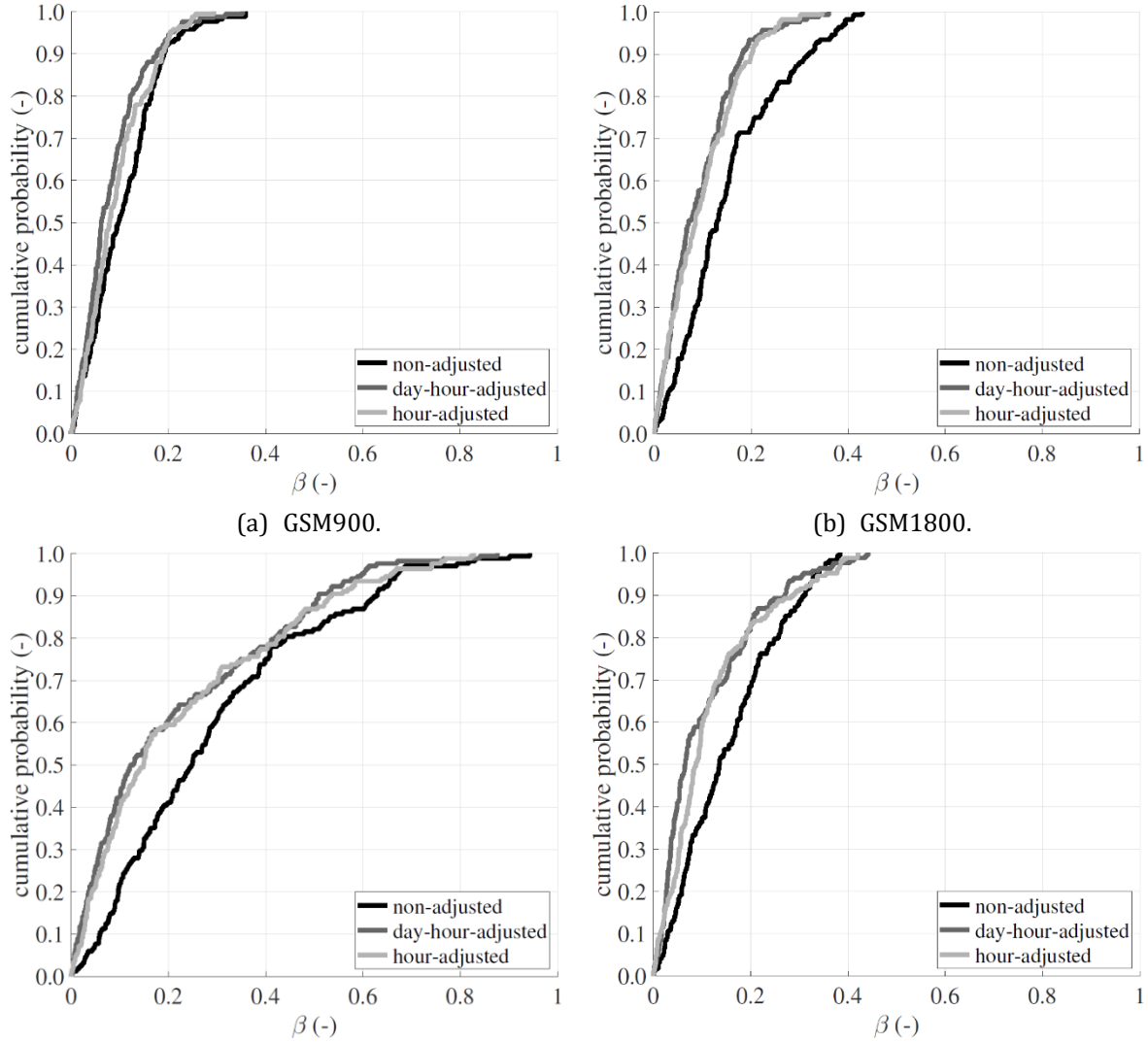

(a) GSM900. (b) GSM1800.

(c) UMTS. (d) Total.

Figure 7: CDFs of the temporal bias β introduced in the interpolation models for three telecommunications downlink signals (+ the total field) by using non-adjusted, day-hour-adjusted, or hour-adjusted measurement values

*Table 1: Median temporal bias **β** introduced in the interpolation model using non-, hour-, and day-hour adjusted measurement values.*

Signal	**Temporal bias β (-)**		
	Non-adjusted	Hour-adjusted	Day-hour-adjusted
GSM900	0.10	0.08	0.06
GSM1800	0.13	0.09	0.07
UMTS	0.25	0.15	0.12
Total	0.14	0.09	0.06
Average	0.16	0.10	0.08

It is clear that using temporal profiles to rescale measurements to the correct time significantly reduced the temporal bias introduced in the model. In Figure 7, the CDFs of the temporal bias for adjusted models are shifted to the left, indicating the higher probability of lower bias. For

example, for UMTS, the median bias β is reduced from 0.25 (non-adjusted) to 0.15 (hour-adjusted) to 0.12 (day-hour-adjusted) (Table 1). The day-hour-adjusted models clearly offer the best results (on average 50% improvement; see also Figure 7 and Table 1), though using the hour profiles offered a reasonable improvement as well (on average 38% improvement; see also Figure 7 and Table 1). Of the three signals, the temporal bias as well as the potential reduction was the highest for UMTS, which follows the observation that the average variation of E_{UMTS} over a day was larger than those of the GSM bands. This behaviour indicates a larger dependency on the UMTS network, especially during peak hours (around noon and 7pm – Figures 4 and 5).

III.3 Strengths & Limitations

For this study, a tremendous amount of spatio-temporal RF-EMF measurement data were collected in a relatively small area. As it is unlikely for measurement-based studies to have such a wealth of information at this spatio-temporal resolution, the temporal profiles were averaged over all measurement locations, and it was found that this location-aggregated profile was already useful. Moreover, even though measurements were optimally adjusted for both the hour and the day of the week (improvement of up to 50%), using mere hour-adjusted values reduced the bias by at least 20% and up to 40%, indicating that a simple adjustment for the measurement hour can result in a more accurate *spatio-temporal* model of the RF-EMF exposure.

All measurements were performed outdoors and only telecommunications downlink bands were considered. As discussed in previous studies (Aerts et al., 2013a; 2013b; 2016), a large part of the human RF-EMF exposure coming from indoor and personal devices was disregarded, as well as broadcast antennas. However, in (Manassas et al., 2012), the short-term temporal variation of environmental RF-EMF due to broadcast antennas was found to be about 40% lower, and in (Aerts et al., 2013a), it was observed that EMF from broadcast networks contributed significantly less to the total environmental exposure compared to telecommunications downlink signals.

Furthermore, the antenna in the measurement device used in this study is a vertically polarized monopole, meaning that the exposimeter measured only one component of the electric field. Moreover, additional uncertainty resulted from averaging the captured values over one-hour intervals. However, this study focused less on the absolute value of the exposure, but rather on the relative improvement of the exposure model when rescaling the used values based on their measurement instant. In addition, an averaging interval of one hour was used here as per practical considerations. In future research, an optimal averaging interval will be determined using a data set of higher temporal resolution.

Next to a dedicated sensor network such as presented in (Diez et al., 2014), there exist a few other measurement setups that can be used for temporal RF measurements, e.g., an exposimeter, worn

by a test subject (Frei et al., 2009; Bolte and Eikelboom, 2012; Urbinello et al., 2014) or placed at a certain location (Vermeeren et al., 2013), a broadband field meter with logging capability, secured to a tripod, or a spectrum analyser setup (Verloock et al., 2014; Joseph and Verloock, 2010). Though the measurement accuracy of these setups (especially with an SA) would be higher, all of them have to be supervised or placed indoors, which is a huge burden or their applicability.

Finally, although the authors are confident of the overall usefulness of temporal profiles for resource-poor spatio-temporal exposure characterization, it is challenging to extrapolate the band-specific results to other geographic areas, as networks and frequency band use are very likely to differ. For example, frequency bands that were initially used for traditional second generation (2G) technology (GSM) may now have been 'refarmed' to accommodate LTE bands.

IV Conclusions

Due to short-term variation over a day or over a week in environmental RF-EMF, measurements performed at different moments during this time can introduce a temporal bias in surrogate models of the RF-EMF exposure such as created in the previous chapters. To help mitigate this bias, temporal profiles can be created, i.e., average trends of the electric-field strength over a certain period of time, and used to rescale the available samples to the correct moment of assessment. In this study, a tremendous amount of spatio-temporal measurement data in three frequency bands used for telecommunications (GSM900, GSM1800, and UMTS) was analysed that was gathered in the SmartSantander Internet-of-Things network. The temporal variation of the signals within the area was contained in either day-hour profiles (i.e., a different profile for each weekday) or simple hour profiles.

It was found that, by rescaling measurements taken at different moments to the same instance of time, a reduction of the temporal bias by up to 40% can be achieved when adjusting only for the hour, and 52% when also adjusting for the day of the week (both for UMTS). The mitigation worked best for UMTS because of its smoother and more outspoken temporal variation during a day. Finally, the work presented in this study indicates that the methodologies used in previous studies (Aerts2013a, Aerts2013b) should include time, either as a fully-fledged extra dimension (next to x and y) which is brought into the smart-sampling methodology, or through long-term temporal measurements at one or more locations within the area to obtain an area-averaged temporal profile. This as well as the validation of the findings reported here in other cities and environments will be the subject of future research.

Acknowledgments

This study was financed by the French Agency for Food, Environmental and Occupational Health & Safety (ANSES) and performed within the AMPERE (Advanced MapPing for the residential ExposuRE to RF-EMF sources) project. Sam Aerts is a Post-Doctoral Fellow of the FWO-V (Research Foundation - Flanders, Belgium).

References

Aerts S., Deschrijver D., Joseph W., Verloock L., Goeminne F., Martens L, and Dhaene T. 2013a. *Exposure assessment of mobile phone base station radiation in an outdoor environment using sequential surrogate modeling.* Bioelectromagnetics 34:300–311.

Aerts S., Deschrijver D., Verloock L., Dhaene T., Martens L., and Joseph W. 2013b. Assessment of outdoor radiofrequency electromagnetic field exposure through hotspot localization using kriging-based sequential sampling. Environ. Res. 126:184–191.

Baliatsas C., Bolte J. F. B.,Yzermans J., *et al.* 2015. *Actual and perceived exposure to electromagnetic fields and non-specific physical symptoms: an epidemiological study based on self-reported data and electronic medical records.* Int. J. Hyg. Environ. Health 218(3):331–44.

Bolte J. F. B. and Eikelboom T. 2012. *Personal radiofrequency electromagnetic field measurements in the Netherlands: Exposure level and variability for everyday activities, times of day and types of area.* Environ. Int. 48C:133–142.

Cucurachi S., Tamis W. L. M., Vijver M. G., *et al*. 2013. *A review of the ecological effects of radiofrequency electromagnetic fields (RF-EMF).* Environ. Int. 51:116–140.

Diez L. F., Anwar S. M., De Lope L. R. , *et al.* 2014. *Design and integration of a low-complexity dosimeter into the smart city for EMF assessment.* EuCNC 2014 - European Conference on Networks and Communications.

Frei P., Mohler E., Neubauer G., et al. 2009. Temporal and spatial variability of personal exposure to radio frequency electromagnetic fields. Environ. Res. 109(6):779–785.

Gotsis A., Papanikolaou N., Komnakos D., Yalofas A., and Constantinou P. 2008. *Non-ionizing electromagnetic radiation monitoring in Greece.* Ann. Telecomm. 63(1-2):109–123.

International Commission on Non-Ionizing Radiation Protection (ICNIRP). 1998. *Guidelines for limiting exposure to time-varying electric, magnetic, and electromagnetic fields (up to 300 GHz).* Health Phys. 74(4):494–522.

Joseph W., Verloock L., Tanghe E., and Martens L. 2009. *In-situ measurement procedures for temporal RF electromagnetic field exposure of the general public.* Health Phys. 96(5):529–542.

Joseph W. and Verloock L. 2010. *Influence of mobile phone traffic on base station exposure of the general public.* Health Phys. 99(5):631–638.

Manassas A., Boursianis A., Samaras T., and Sahalos J. N. 2012. *Continuous electromagnetic radiation monitoring in the environment: analysis of the results in Greece.* Radiat. Prot. Dosim. 151(3):437–442.

Mahfouz Z., Gati A., Lautru D., *et al.* 2012. *Influence of traffic variations on exposure to wireless signals in realistic environments*. Bioelectromagnetics, 33(4):288–297.

Mahfouz Z., Verloock L., Joseph W., *et al*. 2013. *Comparison of temporal realistic telecommunication base station exposure with worst-case estimation in two countries.* Radiat. Prot. Dosim. 157(3):331–338.

Miclaus S., Bechet P., and Gheorghevici M. 2013. *Long-term exposure to mobile communication radiation: An analysis of time-variability of electric field level in GSM900 downlink channels.* Radiat. Prot. Dosim. 154(2):164–173.

Oliveira C., Sebastijo D., Carpinteiro G., *et al.* 2007. *The moniT Project: Electromagnetic Radiation Exposure Assessment in Mobile Communications.* IEEE Antennas Propag. 49(1):44–53.

Rowley J. T. and Joyner K. H. 2012. *Comparative international analysis of radiofrequency exposure surveys of mobile communication radio base stations. J*. Expo. Sci. Environ. Epidemiol. 22(3):304–15.

Troisi F., Boumis M., and Grazioso P. 2008. *The Italian national electromagnetic field monitoring network.* Ann. Telecomm. 63(1-2):97–108.

Tomitsch J. and Dechant E. 2015. Exposure to electromagnetic fields in households – Trends from 2006 to 2012. Bioelectromagnetics, 36(1):77–85.

Urbinello D., Joseph W., Verloock L., Martens L., and Röösli M. 2014. *Temporal trends of radio-frequency electromagnetic field (RF-EMF) exposure in everyday environments across European cities*. Environ. Res. 134C:134–142.

Verloock L., Joseph W., Goeminne F., *et al.* 2014. *Temporal 24-hour assessment of radio frequency exposure in schools and homes.* Measurement, 56:50–57.

Vermeeren G., Markakis I., Goeminne F., *et al.* 2013. *Spatial and temporal RF electromagnetic field exposure of children and adults in indoor micro environments in Belgium and Greece.* Prog. Biophys. Mol. Biol. 113(2):254–263.